iScience

CellPress
OPEN ACCESS

Article

Icaritin inhibits CDK2 expression and activity to interfere with tumor progression

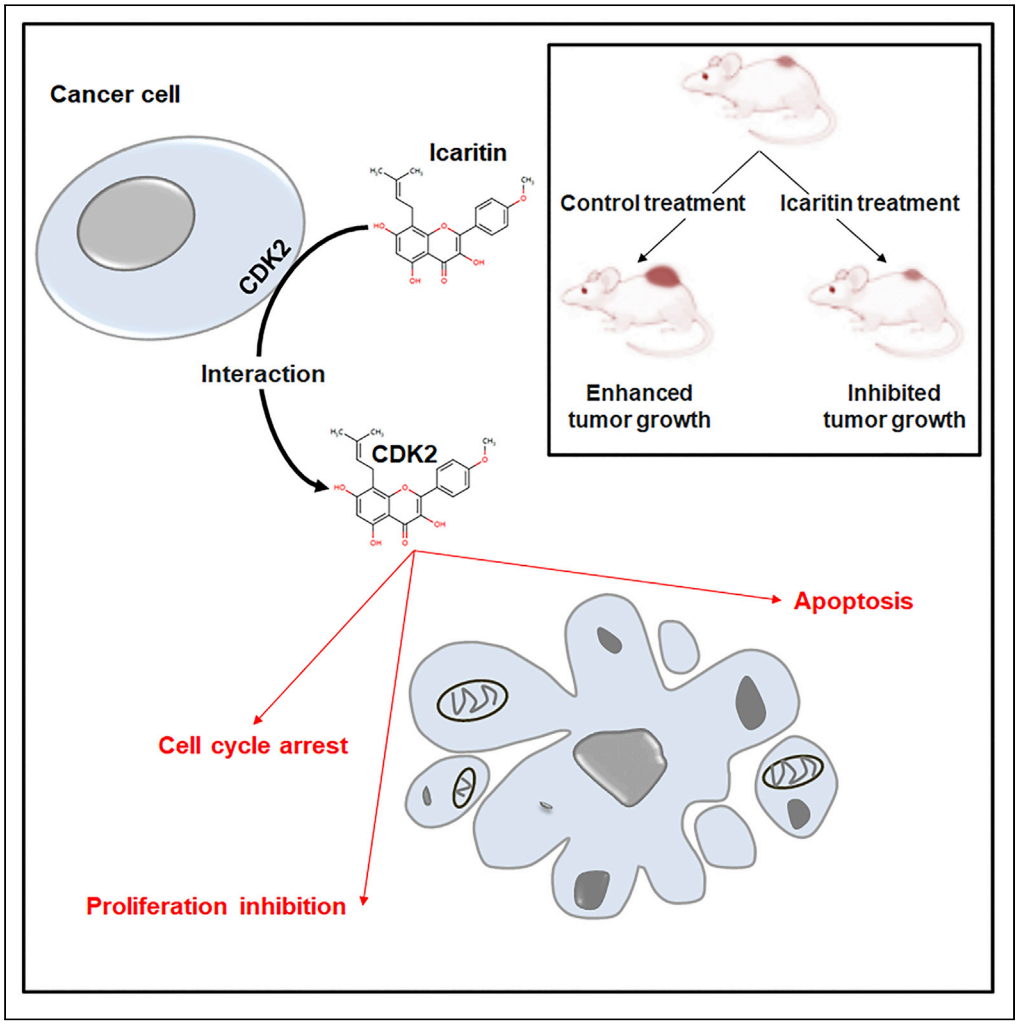

Chao Zhang, Xin Wang, Chuanbao Zhang

zc_mdy@163.com (C.Z.)
cbzhang@nccl.org.cn (C.Z.)

Highlights

Icaritin can interact with CDK2 and affect the biological role of CDK2

Icaritin inhibits the formation of CDK2/cyclin E complex and the activity of CDK2

Icaritin enhance the inhibitory effect of P27 on CDK2

Icaritin regulates tumor cell proliferation and apoptosis in a CDK2-dependent manner

Zhang et al., iScience 25, 104991
September 16, 2022 © 2022 The Author(s).
https://doi.org/10.1016/j.isci.2022.104991

iScience

CellPress
OPEN ACCESS

Article

Icaritin inhibits CDK2 expression and activity to interfere with tumor progression

Chao Zhang,[1,3,*] Xin Wang,[2] and Chuanbao Zhang[1,*]

SUMMARY

Icaritin has shown antitumor activity in a variety of human solid tumors and myeloid leukemia cells. However, the direct target of icaritin and the underlying mechanisms remain unclear. In our study, CDK2 was found to be a direct target of icaritin in tumor cells. On one hand, icaritin interacted with CDK2 and interfered with CDK2/CyclinE complex formation, resulting in downregulation of CDK2 activity as illustrated with attenuated phosphorylation of FOXO1, Rb, and P27, and E2F/Rb dissociation. On the other hand, icaritin reduced the stability and translation efficiency of CDK2-mRNA by modulating microRNA-597 expression. To be of functional importance, icaritin inhibited proliferation and promoted apoptosis of tumor cells *in vitro* and *in vivo*, which was consistent with CDK2 inhibitors—k03861. Our data revealed CDK2 as the direct target of icaritin for its antitumor effects, which may suggest new therapeutics of icaritin or combinational therapeutics involving both icaritin and CDK2 inhibitors for cancers.

INTRODUCTION

Cancer represents a leading cause of death in almost all countries of different income levels. In 2020, the number of new cases for 36 types of cancer in 185 countries worldwide was estimated to be 19.3 million, while the number of cancer-related death was about 10 million, both of which are still increasing by years (Siegel et al., 2017, 2019; Sung et al., 2021). The global odds of developing a type of cancer during a lifetime (age 0–79 years) were about 1 in 3 for men and 1 in 5 for women. In the disability-adjusted life-years caused by cancer, 98% came from years of life lost, while the percentage for years lived with disability was only 2% (Global Burden of Disease Cancer et al., 2018). Therefore, developing effective therapeutic strategies for cancer is urgently required. One hallmark of cancer is aberrant cell cycle activity, which is characterized by increased expression of cyclins or cyclin-dependent kinases (CDKs) and/or decreased levels of endogenous CDK inhibitors such as CIP/KIP (CDK interacting protein/kinase inhibitor protein) family. (Otto and Sicinski, 2017; Roskoski, 2019).

Cell cycle progression is regulated by checkpoint control and sequential activation of CDKs to prevent premature or inappropriate progression to the next phase before successful completion of the current one (Leal-Esteban and Fajas, 2020). Among them, CDK 1, 2, 4, and 6 play fundamental roles in cells passing through the checkpoint, which showed highly increased activities in cancer cells (Icard et al., 2019), and CDKs are considered attractive targets in cancer therapy (Sanchez-Martinez et al., 2019; Tadesse et al., 2019a). Palbociclib, ribociclib, and abemaciclib are FDA approved CDK4/6 inhibitors for the treatment of breast cancer, suggesting the feasibility of the CDK inhibitor treatment approach (Spring et al., 2020). Compared with CDK4/6, which has narrow substrate specificity, CDK1 and CDK2 show wider specificity and catalyze the phosphorylation of dozens of proteins (Spring et al., 2020; Tadesse et al., 2019b). CDK2 is activated by forming complex with cyclin E, which subsequently catalyzes phosphorylation retinoblastoma protein (Rb), promoting the release and activation of transcription factor E2F, leading to biosynthesis of dozens of proteins necessary for cell cycle progression and successful G1/S phase transition (Leal-Esteban and Fajas, 2020; Otto and Sicinski, 2017; Roskoski, 2019). In normal cells, $P27^{Kip1}$ (P27), a member of the CIP/KIP family, blocks cell proliferation through the inhibition of CDK2 (Hauck et al., 2008), while in tumor cells, hyperactivated CDK2 could phosphorylate P27 at Thr187 and induce its ubiquitination degradation, further prompting cell cycle progression in a positive feedback manner(Shin et al., 2002; Starostina and Kipreos, 2012). Moreover, in tumors induced by c-Myc overexpression, activated CDK2 phosphorylates c-Myc at Ser62 to block recognition and ubiquitination by the SCF ubiquitin-protein-ligase complex, thereby preventing c-Myc degradation (Hydbring et al., 2010). The findings that CDK2 mediates the phosphorylation of

[1]National Center for Clinical Laboratories, Beijing Hospital, National Center of Gerontology, Institute of Geriatric Medicine, Chinese Academy of Medical Sciences, P. R. China

[2]Center for Endocrine Metabolism and Immune Diseases, Beijing Luhe Hospital, Capital Medical University, Beijing Key Laboratory of Diabetes Research and Care, Beijing, China

[3]Lead contact

*Correspondence: zc_mdy@163.com (C.Z.), cbzhang@nccl.org.cn (C.Z.)

https://doi.org/10.1016/j.isci.2022.104991

This is an open access article under the CC BY-NC-ND license (http://creativecommons.org/licenses/by-nc-nd/4.0/).

androgen, estrogen, and progesterone receptors and increases their transcriptional activities makes CDK2 an attractive target in hormone-dependent breast and prostate cancer (Jorda et al., 2018; Pierson-Mullany and Lange, 2004; Yin et al., 2018). CDK2 was not only involved in cell proliferation but also in apoptosis. Silencing of CDK2 using RNAi reduced the phosphorylation of FOXO1 at Ser249 inhibitory sites, which allowed FOXO1 to become transcriptionally active and trigger apoptosis via upregulation of numerous pro-apoptotic proteins such as FasL, TRAIL, and Bim (Huang et al., 2006; Huang and Tindall, 2007b). Given the importance of overactivated CDK2 in tumorigenesis and the fact that CDK2 mutations are rarely found in human cancers, development of selective inhibitors for CDK2 is in urgent need to treat specific cancer subtypes.

Icaritin is a hydrolytic product of icariin isolated from the traditional Chinese herbal medicine genus Epimedium, which has shown multiple pharmacological and biological activities. Icaritin has shown antitumor activity in a variety of human solid tumor and myeloid leukemia cells. It was able to inhibit the proliferation and promote apoptosis of cells from glioblastoma, hepatocellular carcinoma, renal cell carcinoma, lung cancer, ovarian cancer, and osteosarcoma, partially through activating TRAIL or Fas-caspase-3/8 apoptosis pathway (Han et al., 2015; Sun et al., 2015; Wang and Wang, 2014), inhibiting NF-κB or JAK/STAT3 signaling pathway (Li et al., 2013; Mo et al., 2021), inducing cell cycle arrest (Zheng et al., 2014), reducing Bcl-2 expression, and changing Bcl-2/Bax ratio (Li et al., 2015) and other pathways. One intriguing phenomenon is that although icaritin could induce cycle arrest, inhibit tumor cell proliferation, promote necrosis and apoptosis, and alter the expression of multiple proliferation/apoptosis-related genes, its direct molecular targets are still unknown. Through a reverse virtual screening, CDK2 was found likely to be one of the direct targets of icaritin, which might explain the potent effect of icaritin on tumor cell proliferation and apoptosis.

In this study, we uncovered a novel functional role and regulatory mechanism of icaritin on the CDK2-cyclin E formation and CDK2 activation in the cell cycle. Our data show that icaritin interacted with CDK2 and consequently inhibit the formation of CDK2/cyclin E and CDK2 activation, leading to cell cycle arrest and increasing apoptosis of tumor cells.

RESULTS

Icaritin interacted with CDK2 to inhibit the formation of CDK2/cyclin E complex

PyMOL software was used to generate the CDK2 binding pocket and then an autodocking platform to mimic the interaction between icaritin and CDK2 (Figure S1). Icaritin and CDK2 can interact with each other through a C-H bond, conventional hydrogen bond, π-sigma, π-π, and so on, both in human and all species of protein structure databases (PDB: 1JVP, 4ACM) (Figure 1A and Table S1). The amino acid residues accounting for interaction were conserved across species. Surface plasmon resonance was further employed to confirm the interaction between icaritin and CDK2 (Figure 1B). As CDK2 is critical for the cell cycle, we thus verified whether the interaction could affect the function of CDK2. To obtain the optimal concentration, we tested different concentrations of icaritin (0–40 μM), and the relative inhibition rate of PLC and HT-29 cells was analyzed by the cell viability assay. IC50 (20 μM) was selected for further experiments (Figure S2). Both icaritin and k03861 (an inhibitor of CDK2 (Alexander et al., 2015; Kozyrska et al., 2022)) could inhibit the formation of the CDK2/cyclin E complex and thus inhibit the dissociation of E2F/Rb (Figures 1C and 1D). Consistently, the phosphorylations of FOXO1, Rb, and P27 were obviously decreased, which was restored by overexpression of CDK2 (Figure S3; Figures 1E and 1F). Together, these results suggest that icaritin might reduce the phosphorylations of FOXO1, Rb, and P27 by inhibiting the formation of the CDK2/cyclin E complex and activation of CDK2. Meanwhile, the expression of apoptosis-related genes, FasL, Bim, and TRAIL, downstream of transcritional targets of FOXO1, was significantly increased upon icaritin treatment (Figure S4).

Icaritin inhibits CDK2 expression by increasing the expression of miR-597

We then investigated whether icaritin also affected the expression of CDK2, cyclin E, FOXO1, and P27. No obvious alterations in the expression of FOXO1 and cyclin E were observed in PLC and HT-29 cells. It was interesting to note that CDK2 showed a significant decrement at both the mRNA and protein levels with icaritin treatment at 36 h, while P27 showed an opposite trend (Figures 2A–2D). Moreover, the changes in P27 and CDK2 expression are the most obvious at 10–20μM. Thus, icaritin can not only interact with CDK2 but also inhibit CDK2 expression. We then investigated the mechanism underlying the inhibitory effect of icaritin on the expression of CDK2. Previous studies have confirmed that miR-597, as an antitumor microRNA, could bind the 3′-UTR of CDK2 in non-small cell lung cancer cells to suppress its expression

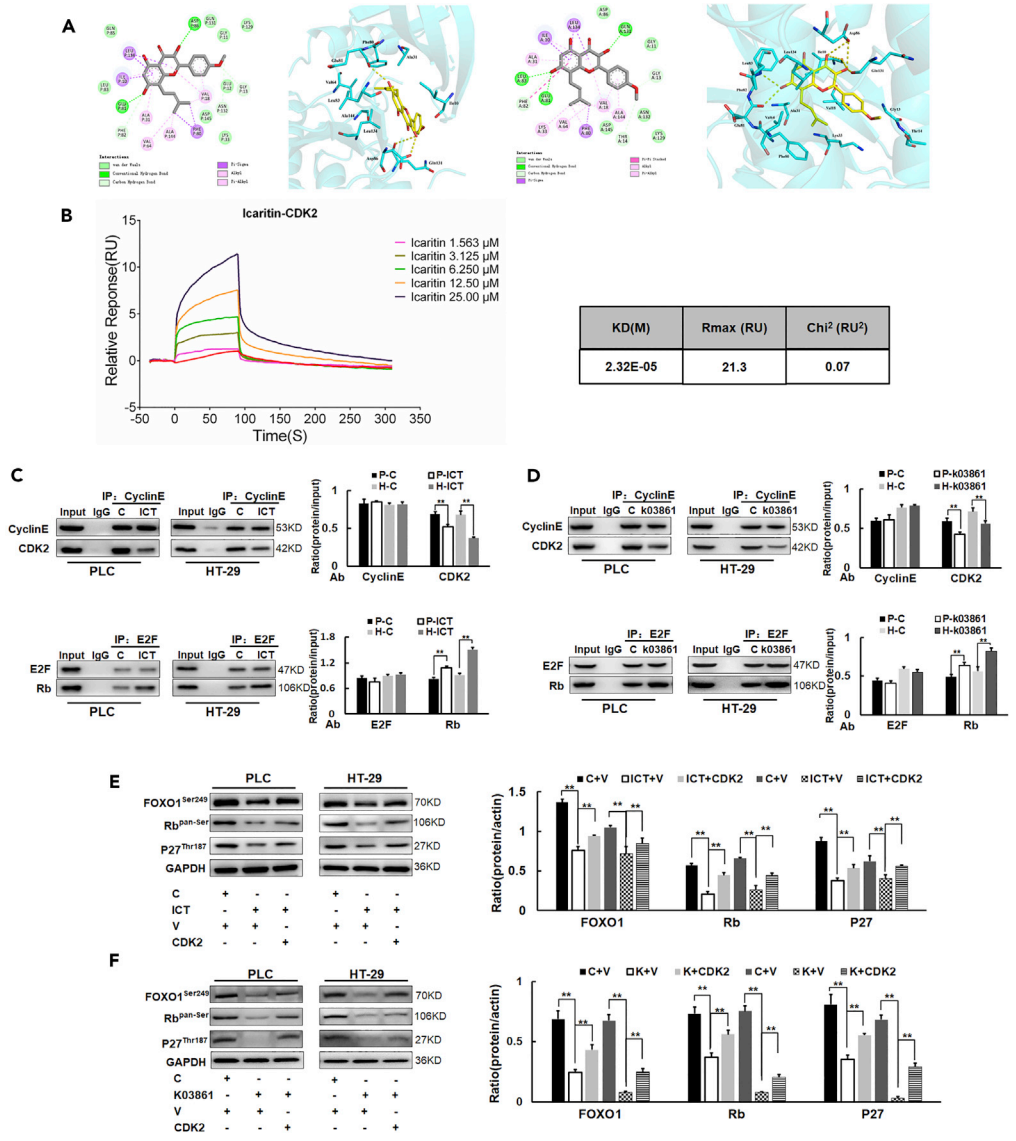

Figure 1. Icaritin inhibits CDK2/cyclin E complex formation and CDK2 activation

(A) Icaritin-CDK2 interaction sites in the pocket.

(B) The interaction between icaritin and CDK2 was examined by surface plasmon resonance.

(C and D) Coimmunoprecipitation analysis of the interaction of CDK2 and cyclin E, Rb, and E2F in PLC and HT-29 cells treated with icaritin and k03861.

(E and F) Western blot analysis on *p*-FOXO1, p-Rb, and p-P27 upon treatment with and k03861 alone or together with CDK2 transfection. C: DMSO control; ICT: Icaritin; V: empty vector; CDK2: transfection with pcDNA3.1-*CDK2*; k03861: an inhibitor of CDK2. These experiments were repeated at least three times. *$p < 0.05$; **$p < 0.01$.

(Yu et al., 2020). Consistent with previous findings, transfections of miR-597 mimics or inhibitors into PLC and HT-29 cells for 36 h dramatically reduce or increase the level of CDK2 protein, respectively (Figure 2E). The miR-597 inhibitor specifically reduced the levels of endogenous miR-597 (Figure 2F). More importantly, icaritin led to significant increase in miR-597 levels (Figure 2G), suggesting the involvement of miR-597 in icaritin-mediated suppression of CDK2.

Icaritin triggers G1/S arrest and apoptosis in tumor cells

To further confirm the functional significance of the interaction between icaritin and CDK2 in the cell cycle, cells were treated with icaritin followed by flow cytometric analyses and confocal laser microscopy.

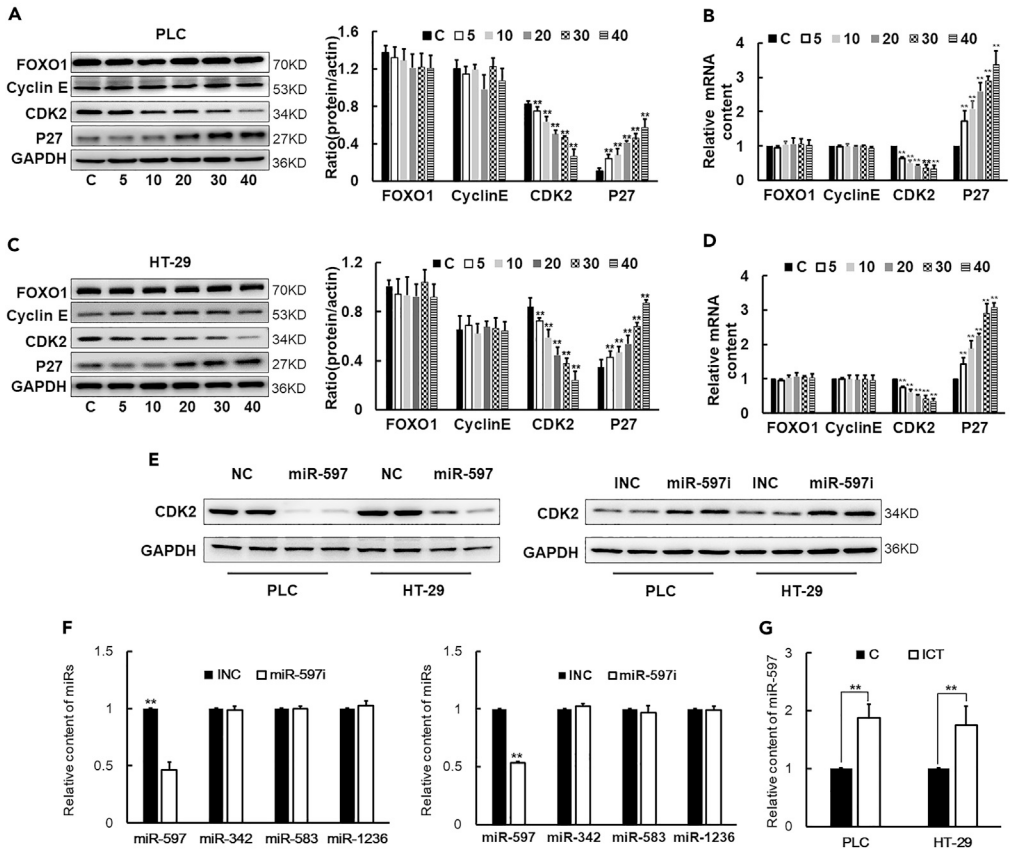

Figure 2. Expression alterations of FOXO1, CDK2, cyclin E, and P27 after icaritin treatment for 36 h in PLC and HT-29 cells

(A and B) Western blot and RT-qPCR analyses on the expression of FOXO1, CDK2, cyclin E, and P27 in PLC cells with icaritin treatment.

(C and D) Western blot and RT-qPCR analyses on the expression of FOXO1, CDK2, cyclin E, and P27 in HT-29 cells with icaritin treatment.

(E) Effect of miR-597 mimic or inhibitor on CDK2 protein expression at 36 h after transfection.

(F) Effects of miR-597 mimics (50 pmol/well) or inhibitors (50 pmol/well) on the level of miR-597, miR-342, miR-583, and miR-1236 at 36 h after transfection. NC: negative control for mimic. INC: negative control for inhibitor.

(G) Effects of icaritin on miR-597 expressions post 36 h treatment. These experiments were repeated at least three times. Data represent the mean ± SD of three samples. **$p < 0.01$ as compared with controls.

As shown in Figures 3A and 3C, compared with the control group, the G1/S transition of icaritin-treated cells was significantly arrested and the proportion of S phase cells was decreased by 45.8% and 47.9% in PLC and HT-29 cells, respectively. Meanwhile, a dramatic reduction in proliferation was observed in both PLC (26.3%) and HT-29 cells (37.6%) (Figures 3E and 3G). On the contrary, overexpression of CDK2 drastically increased the percentage of cells in the S phase increased by 24.4% and 29.3% in PLC and HT-29 respectively, accompanied with higher proliferation rate (by 25.2% in PLC while by 20.1% in HT29 cells) (Figures 3B and 3D). The heat density figures of cell proliferation showed similar results to the EdU incorporation experiments (Figure S5A). These results suggest that icaritin can attenuate G1/S transition possibly through complexing with CDK2, thus inhibiting proliferation of tumor cells. Furthermore, flow cytometric analysis also showed that treatment with icaritin resulted in an apparent increase of apoptotic cells, the percentage of which were increased by 111.6 and 102.1% in PLC and HT-29 cells, respectively (Figure 3E). Nucleus pyknosis, karyorrhexis, and karyolysis were also observed in those apoptotic cells (Figure S5B). More importantly, the percentages of apoptotic cells were decreased by 32.4% and 42.5% and the nuclear morphology was partially restored upon CDK2 overexpression (Figures 3F and S5B). The inhibitory effect of icaritin on tumor cell proliferation was further confirmed in hepatoma cells,

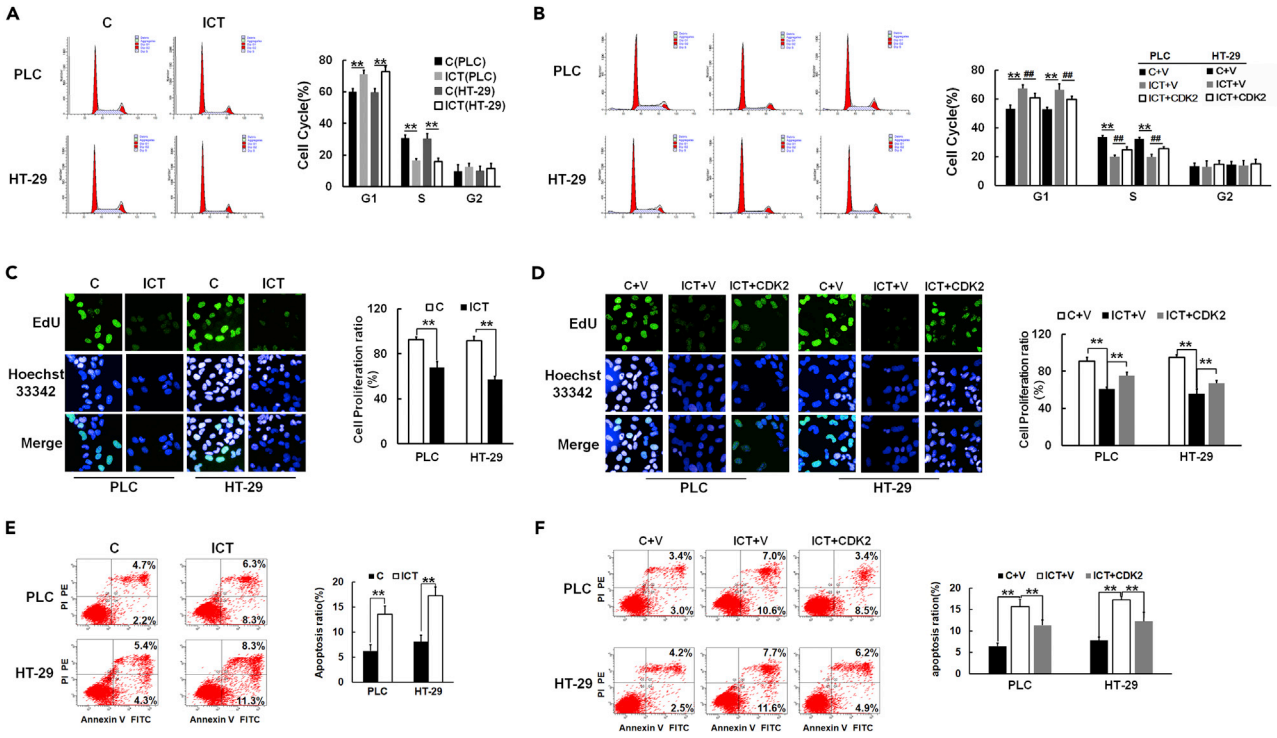

Figure 3. Effects of icaritin on cell cycle, proliferation, and apoptosis

(A) Cell cycle analyses with flow cytometry in PLC and HT-29 cells with icaritin treatment.

(B) Effects of overexpression of CDK2 on icaritin-induced cell cycle arrest.

(C and D) Effects of icaritin and CDK2 on proliferation in PLC and HT-29 cells. Proliferative cells were labeled in green, the nucleus in blue, and the statistical analysis by averaging the numbers of proliferative cells per low-power field (LPF) for 5 fields in each experiment.

(E) Effects of icaritin on cell apoptosis were analyzed by flow cytometry at 36 h post-treatment in PLC and HT-29 cells.

(F) Effects of CDK2 on apoptosis in PLC and HT-29 cells treated with icaritin. The image is representative of three independent experiments.

prostate cancer cells, breast cancer cells, colorectal cancer cells, and cervical cancer cells, suggesting a broad spectrum of inhibition (Figure S5C).

Icaritin inhibits xenograft tumor growth in the cell-derived xenograft model

The antitumor activity of icaritin was further testified in an *in vivo* cell-derived xenograft (CDX) model. The growth of xenograft tumors in icaritin-treated mice was much more slower than in the control mice in both PLC and HT-29 CDX models (Figure 4A). Compared with control groups, the weight of tumors was much lighter in icaritin-treated groups. However, there was no significant difference in body weight between the two groups (Figure S6). The expression of CDK2 and P27 was also evaluated with immunohistochemical staining. In both PLC and HT-29 xenograft tumor tissues, expression of CDK2 was decreased while that of P27 increased significantly, consistent with the results of *in vitro* experiments (Figure 4B). Meanwhile, apoptosis was evaluated by TUNEL assay, and much more apoptotic TUNEL-positive cells were identified in both tumor tissue slides from the icaritin-treated groups compared with those from the control group (Figure 4C). As another manifestation of drug (icaritin) therapy, control tumor tissues showed no observable structural damage, comparable with normal tissue. In contrast, icaritin-treated tumor tissues displayed infiltration of massive inflammatory cells and extensive cell necrosis (Figure 4D).

Icaritin inhibits the formation of CDK2/cyclin E complex and downstream phosphorylation events *in vivo*

We then analyzed whether icaritin inhibited CDK2/cyclin E complex formation and CDK2 activation in the CDX mice model. As expected, the results *in vivo* were highly consistent with that *in vitro*. Neither PLC group nor HT-29 group showed alteration of expression of FOXO1 and cyclin E at the mRNA and protein levels. Of note, the levels of CDK2 and P27 were apparently decreased and increased with icaritin

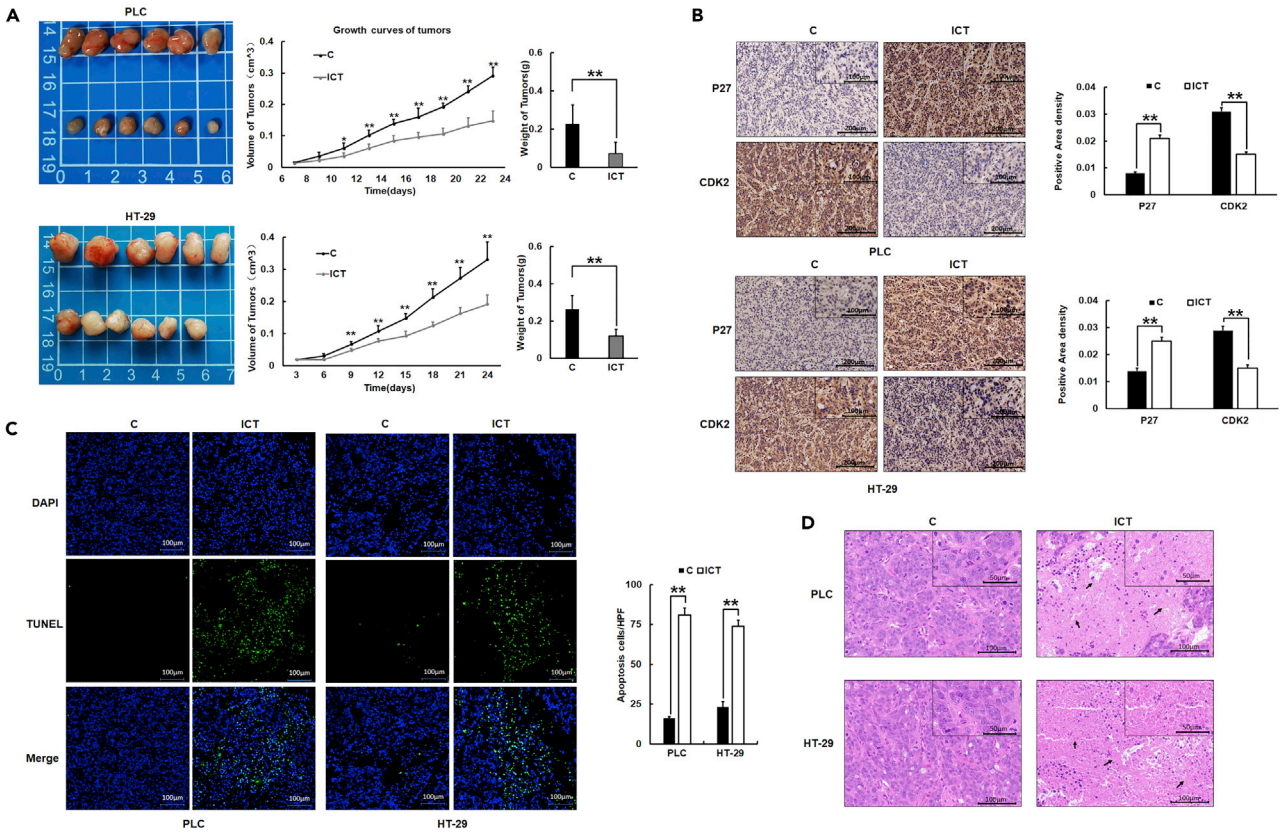

Figure 4. Icaritin inhibits tumor growth in CDX mice. Suspended PLC and HT-29 cells were injected subcutaneously into the armpits of mice, followed with gavage of icaritin for 24 days (every day)

(A) Comparison of xenograft growth rate and weight between two groups.

(B) Expression of CDK2 and P27 was evaluated by IHC and positive area density.

(C) TUNEL analysis of apoptosis. TUNEL-positive cells were green under fluorescence microscopy and quantified from 10 randomly selected fields at ×200 magnification.

(D) Representative histological staining (H&E) of tumor tissue. Results showed representative sample of 10 mice/group. **$p < 0.01$. Data represent the mean ± SD of 10 animals in each group.

treatment, respectively (Figure 5A). To verify the role of icaritin in regulating the CDK2/cyclin E formation and CDK2 activation, proteins that were phosphorylated by activated CDK2 were detected. Icaritin-treated tumor cells showed much less phosphorylation of FOXO1 at Ser-249 and P27 at Thr 187 and Rb compared with the control group in both PCL and HT-29-formed tumor tissues (Figure 5B). The decrease in FOXO1 phosphorylation also resulted in a significant increase in the expression of its downstream FasL, Bim, and TRAIL (Figure S7). Tissue protein coimmunoprecipitation further confirmed that icaritin inhibited the formation of the CDK/cyclin E complex, thereby weakening the release of E2F from the E2F/Rb complex (Figure 5C). Meanwhile, consistent with the regulation of CDK2 expression by miR-597, icaritin-treated cells showed upregulation of the miR-597 compared with the control group (Figure 5D).

DISCUSSION

In this study, we demonstrate that (1) icaritin inhibits the expression of CDK2 by increasing the level of miR-597; (2) icaritin inhibits the formation of CDK2/cyclin E complex and the activity of CDK2; (3) icaritin promotes the expression while attenuates the phosphorylation of P27, thereby enhances the inhibitory effect of P27 on CDK2; and (4) icaritin regulates tumor cell proliferation and apoptosis in a CDK2-dependent manner. Our results highlight the importance of icaritin in orchestrating CDK2 activation, tumor cell proliferation, and apoptosis. To the best of our knowledge, this is the first study to document that CDK2 is the direct target of icaritin, which regulates CDK2-mediated tumor proliferation and apoptosis.

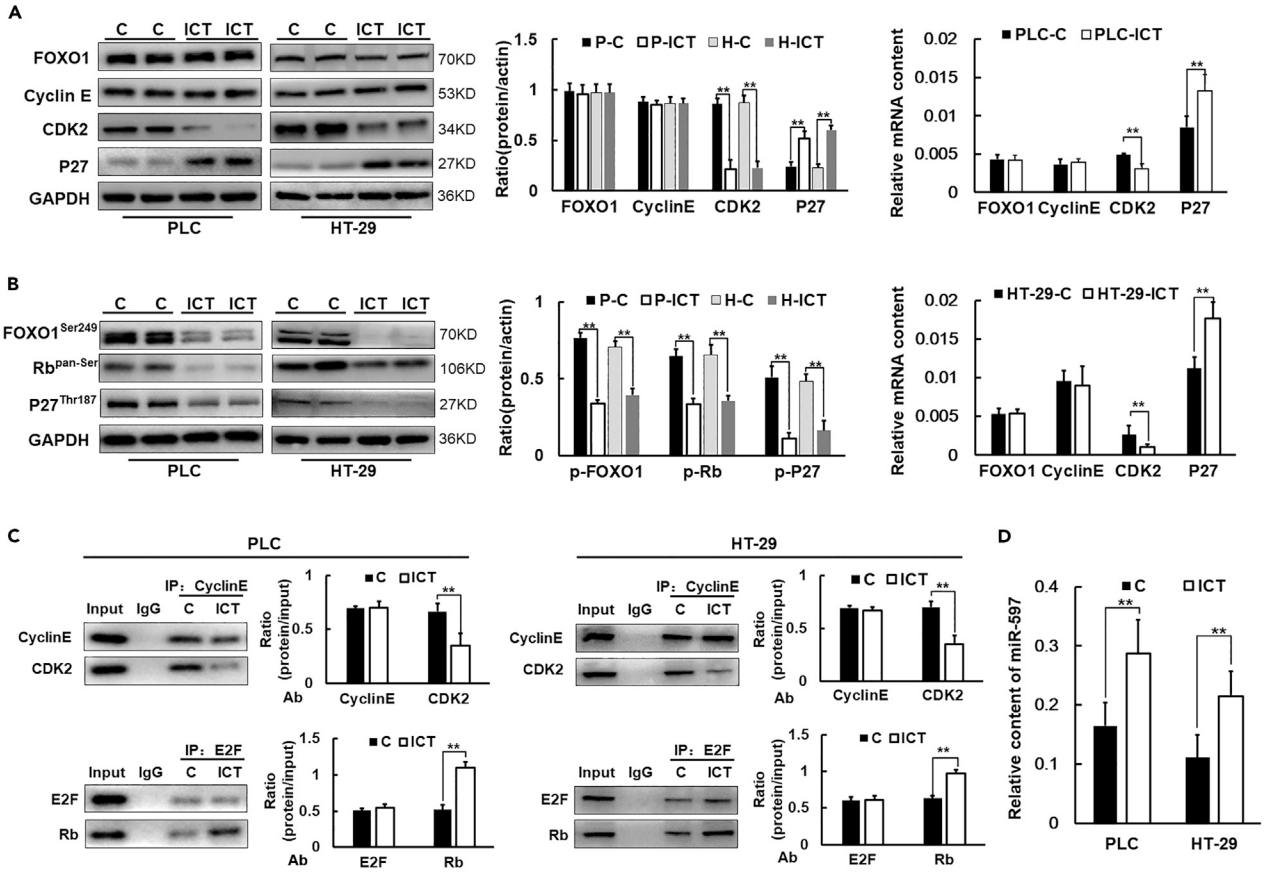

Figure 5. Icaritin inhibits CDK2/cyclin E complex formation and CDK2 activation in tumor tissues

(A) Western blot and RT-qPCR of FOXO1, CDK2, cyclin E, and P27.

(B) Western blot analyses and relative density ratio of *p*-FOXO1, p-Rb, and p-P27.

(C) Coimmunoprecipitation analyses of the interaction between CDK2 and cyclin E, Rb, and E2F in tumor tissues.

(D) The expression of miR-597 in control and icaritin-treated tumor tissues. Representative of three experiments. *$p < 0.05$; **$p < 0.01$.

Interaction between icaritin and CDK2 directly inhibits the formation of CDK2/cyclin E and activation of CDK2, thereby affecting the downstream molecular events: dissociation of E2F and Rb and phosphorylation of P27 and FOXO1. Overexpression of CDK2 alleviated the inhibition of icaritin, suggesting the specificity of icaritin on CDK2 to function (Figures 1 and 2). To be of functional significance, inhibition of CDK2 by icaritin resulted in cell cycle arrest, decreased proliferation, and increased apoptosis, which could also be rescued by overexpression of CDK2 (Figure 3). Moreover, using the CDX model, we found that icaritin inhibited the formation of CDK2/cyclin E, the dissociation of E2F and Rb, and the phosphorylation levels of P27 and FOXO1, as well as significant inhibition in the tumor growth and an increase in xenograft tissue damage and apoptosis (Figures 4 and 5). All the above results suggest that the regulation of icaritin on CDK2 by interacting with it plays a pivotal role in cell proliferation and apoptosis.

Current researches on the tumor suppression effect of icaritin mainly focus on the indirect effects rather than on its direct targets, such as activation of TRAIL or Fas-caspase-3/8 apoptosis pathway, inhibition of NF-κB or JAK2/STAT3 pathway, or induction of cell cycle arrest (Han et al., 2015; Sun et al., 2015; Yang et al., 2019; Zheng et al., 2021). How those changes occur has not been explored. In the early G1 phase, CDK4/6 initiates the phosphorylation of Rb, resulting in partial dissociation of E2F from Rb, which in turn initiates cyclin E expression. Subsequently, cyclin E binds to and activates CDK2, which further induces hyperphosphorylation of Rb and complete dissociation of Rb/E2F complex, leading to S phase gene expression and G1/S transition. Interestingly, cyclin E expression remained unchanged upon icaritin treatment in our results, suggesting that icaritin did not target CDK4/6. Activated CDK2 could phosphorylate the inhibitory site Ser249 of FOXO1, thereby inhibiting its transcriptional activity (Huang et al., 2006;

Huang and Tindall, 2007a). Icaritin could reverse this effect and promote the transcriptional activity of FOXO1, thus promoting the expression of TRAIL, FasL, and Bim regulated by FOXO1, which explains why icaritin could activate TRAIL and caspase-dependent apoptotic pathways. Tumor suppressor P27, a potent inhibitor of cell growth and division, could inhibit CDK2 activity under normal conditions (Bury et al., 2021). In some tumors, CDK2 activity is enhanced following reduced expression of P27 (Liang et al., 2002). Genetic deletion of P27 in mice results in multi-organ hyperplasia and tumor development. In cancer patients, increased degradation of P27 correlates with aggressive tumors and poor prognosis (Aarts et al., 2013; Otto and Sicinski, 2017). Activated CDK2 could phosphorylate P27 on Thr187 to promote its ubiquitination and proteasomal degradation (Razavipour et al., 2020). Icaritin could increase the expression of P27 and suppress the phosphorylation of P27 at Thr187. Collectively, these mechanisms establish a positive feedback loop, amplifying the inhibitory effect of P27 through the inactivation of CDK2. Moreover, at the end of mitosis, the cell decides either to enter into the next cell cycle by immediately building up CDK2 activity or to a transient G0-like state by suppressing CDK2 activity (Spencer et al., 2013). Thereupon, the negative regulation of icaritin on CDK2 can promote the overproliferating cells into quiescence.

The antitumor effect of icaritin has been studied for a long time, but its direct target has not been found. In this study, we used reverse virtual screening technology, protein structure databases, and molecular autodocking software to screen potential targets of icaritin, which was helpful to clarify the new molecular mechanism of antitumor effect of icaritin and discover the possible toxic and side effects (Carvalho et al., 2017; Huang et al., 2018; Kirchmair et al., 2011). Moreover, through reverse virtual screening, we can study possible new targets of existing antitumor drugs and supplement the new mechanisms of antitumor roles, which can target enhanced anticancer effects and greatly reduce the cost of drug development (Saeidnia et al., 2016). The broad functionality of CDK2 in proliferative and prosurvival pathways highlights it as an ideal target for mechanism-based and low-toxicity therapeutic strategies in cancer treatment (Tadesse et al., 2019a). In *KRAS*-mutant lung cancer models, inhibition of CDK2 activity leads to anaphase catastrophe and apoptosis and decreases lung cancer xenograft growth. CDK2 inhibition has been suggested for use in highly aneuploid cancers, since many cancers have aneuploid cells with redundant centrosomes, which may have the potential to extend CDK2 inhibition to other cancers (Kawakami et al., 2018). Moreover, CDK2 inhibition is particularly useful for endocrine therapy-resistant breast cancer. Endocrine resistance occurs in ~30% of patients undergoing endocrine therapy for hormone-dependent breast cancer, and most of these resistant pathways are eventually accompanied by CDK2 activation. Inhibition of CDK2 prevented proliferation of tamoxifen-resistant cells and restored their sensitivity to antiestrogen therapy, suggesting that the possibility of targeting CDK2 against these resistance mechanisms has been established (Johnson et al., 2010). CDK2 is also a key target that provides therapeutic choice for cases with resistance to CDK4/6 inhibitors. However, the specificity of CDK2 inhibitors discovered so far is poor, due to off-target effects (Tadesse et al., 2019a; Wang et al., 2021). Therefore, obtaining highly specific CDK2 inhibitors will be a major progression for new and effective targeted therapies of cancer, especially in those subtypes with CDK2 dependency. In the reverse virtual screening results, icaritin only targets CDK2 and does not interact with other CDKs (Table. S2). Our verification of the direct target and mechanism of icaritin provides new ideas and theoretical guidance for CDK2-specific inhibitors.

Figure 6 depicts the putative molecular mechanisms by which the icaritin may regulate CDK2-mediated proliferation and apoptosis in tumor cells. Activated CDK2-phosphorylated Rb to initiate the S-phase gene synthesis, phosphorylated P27 to weaken the inhibitory effect of P27 on CDK2, and phosphorylated FOXO1 to inhibit TRAIL and FasL triggered apoptosis pathway, respectively (Huang et al., 2006; Kumarasamy et al., 2021; Otto and Sicinski, 2017). This study demonstrates the new pathway of icaritin antitumor effects through combing with CDK2 to inhibit the formation of CDK2/cyclin E and the activation of CDK2. The inhibitory effect of icaritin on CDK2 expression synergistically intensified the suppression of CDK2 activity. Inactivation of CDK2 resulted in significantly reduced phosphorylation of Rb, FOXO1, and P27, leading to cell cycle arrest and increased apoptosis. Moreover, the reduction of P27 degradation and the promotion of P27 expression by icaritin form a positive feedback loop, which greatly enhanced the inhibitory effect of P27 on CDK2.

In conclusion, our data reveal links among icaritin, miR-597, CDK2, P27, and FOXO1 in the proliferative and apoptotic program. We demonstrate that icaritin regulates tumor progression by targeting CDK2. Future studies need to explore how icaritin interacts with CDK2 further, how it regulates P27 expression, and

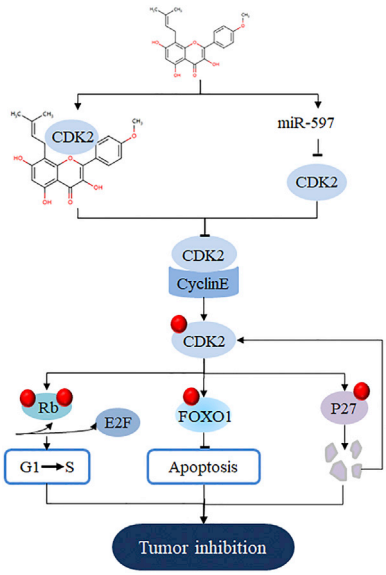

Figure 6. Schematic model of the possible role of icaritin in regulating tumor cell proliferation and apoptosis

whether it affects the formation of CDK2/cyclin A in the S-phase and its relationship with other proliferation/apoptosis factors to enhance the synergistic effect of icaritin in antitumor effects. By identifying the molecular mechanism by which icaritin regulates CDK2-mediated proliferation and apoptosis, our findings provide the rationale for new therapeutic approaches for clinical tumor treatment, as well as a theoretical basis for the development of CDK2-specific inhibitors.

Limitations of the study

Icaritin was slightly soluble in water, and the maximum dissolution capacity in DMSO was about 15 g/L. Considering the toxicity of DMSO, the concentration of DMSO in the drug solvent used for injection should not exceed 1%. In our experiments, the amount of icaritin injected to mice should not exceed 10 mg/kg. If calculated based on this premise, the final concentration of DMSO is 13.3%, which is obviously not suitable for injection. So, the only choice in our study was to dissolve icaritin in corn oil and gavage the mice.

STAR★METHODS

Detailed methods are provided in the online version of this paper and include the following:

- KEY RESOURCES TABLE
- RESOURCE AVAILABILITY
  - Lead contact
  - Materials availability
  - Data and code availability
- EXPERIMENTAL MODEL AND SUBJECT DETAILS
  - Cell lines
  - Animals
- METHOD DETAILS
  - Reverse virtual screening
  - Cell-Derived Xenograft (CDX) model
  - Surface plasmon resonance (SPR)
  - Histology staining
  - Plasmid transfection
  - Reverse transcription and quantitative real-time PCR (RT-qPCR)
  - Western blotting
  - Coimmunoprecipitation (CoIP)
  - Cell nuclei staining for apoptosis
  - Determination of cell viability

- Flow cytometric analysis for apoptosis
- Flow cytometric analysis for cell cycle
- EdU incorporation assay
- TUNEL staining for apoptosis

- QUANTIFICATION AND STATISTICAL ANALYSIS

SUPPLEMENTAL INFORMATION

Supplemental information can be found online at https://doi.org/10.1016/j.isci.2022.104991.

ACKNOWLEDGMENTS

This work was supported by the National Natural Science Foundation of China (No. 82003809) and Beijing Natural Science Foundation (No. 7222157). We thank Wenting Hou and Chenguang Zhang for editorial assistance and Yong Zhao for technical support.

AUTHOR CONTRIBUTION

C. Z. designed the study, analyzed the data, and drafted the manuscript. C. Z. and CB. Z. participated in management of data. X. W. participated in animal model.

DECLARATION OF INTERESTS

The authors declare no competing interests.

Received: June 6, 2022
Revised: July 27, 2022
Accepted: August 16, 2022
Published: September 16, 2022

REFERENCES

Aarts, M., Linardopoulos, S., and Turner, N.C. (2013). Tumour selective targeting of cell cycle kinases for cancer treatment. Curr. Opin. Pharmacol. *13*, 529–535.

Alexander, L.T., Möbitz, H., Drueckes, P., Savitsky, P., Fedorov, O., Elkins, J.M., Deane, C.M., Cowan-Jacob, S.W., and Knapp, S. (2015). Type II inhibitors targeting CDK2. ACS Chem. Biol. *10*, 2116–2125.

Bury, M., Le Calvé, B., Ferbeyre, G., Blank, V., and Lessard, F. (2021). New insights into CDK regulators: novel opportunities for cancer therapy. Trends Cell Biol. *31*, 331–344.

Carvalho, D., Paulino, M., Polticelli, F., Arredondo, F., Williams, R.J., and Abin-Carriquiry, J.A. (2017). Structural evidence of quercetin multi-target bioactivity: a reverse virtual screening strategy. Eur. J. Pharm. Sci. *106*, 393–403.

Global Burden of Disease Cancer Collaboration, Fitzmaurice, C., Akinyemiju, T.F., Al Lami, F.H., Alam, T., Alizadeh-Navaei, R., Allen, C., Alsharif, U., Alvis-Guzman, N., Amini, E., et al. (2018). Global, regional, and national cancer incidence, mortality, years of life lost, years lived with disability, and disability-adjusted life-years for 29 cancer groups, 1990 to 2016: a systematic analysis for the global burden of Disease study. JAMA Oncol. *4*, 1553–1568.

Han, H., Xu, B., Hou, P., Jiang, C., Liu, L., Tang, M., Yang, X., Zhang, Y., and Liu, Y. (2015). Icaritin sensitizes human glioblastoma cells to TRAIL-induced apoptosis. Cell Biochem. Biophys. *72*, 533–542.

Hauck, L., Harms, C., An, J., Rohne, J., Gertz, K., Dietz, R., Endres, M., and von Harsdorf, R. (2008). Protein kinase CK2 links extracellular growth factor signaling with the control of p27(Kip1) stability in the heart. Nat. Med. *14*, 315–324.

Huang, H., and Tindall, D.J. (2007a). CDK2 and FOXO1: a fork in the road for cell fate decisions. Cell Cycle *6*, 902–906.

Huang, H., and Tindall, D.J. (2007b). Dynamic FoxO transcription factors. J. Cell Sci. *120*, 2479–2487.

Huang, H., Regan, K.M., Lou, Z., Chen, J., and Tindall, D.J. (2006). CDK2-dependent phosphorylation of FOXO1 as an apoptotic response to DNA damage. Science *314*, 294–297.

Huang, H., Zhang, G., Zhou, Y., Lin, C., Chen, S., Lin, Y., Mai, S., and Huang, Z. (2018). Reverse screening methods to search for the protein targets of chemopreventive compounds. Front. Chem. *6*, 138.

Hydbring, P., Bahram, F., Su, Y., Tronnersjö, S., Högstrand, K., von der Lehr, N., Sharifi, H.R., Lilischkis, R., Hein, N., Wu, S., et al. (2010). Phosphorylation by Cdk2 is required for Myc to repress Ras-induced senescence in cotransformation. Proc. Natl. Acad. Sci. USA *107*, 58–63.

Icard, P., Fournel, L., Wu, Z., Alifano, M., and Lincet, H. (2019). Interconnection between metabolism and cell cycle in cancer. Trends Biochem. Sci. *44*, 490–501.

Johnson, N., Bentley, J., Wang, L.Z., Newell, D.R., Robson, C.N., Shapiro, G.I., and Curtin, N.J. (2010). Pre-clinical evaluation of cyclin-dependent kinase 2 and 1 inhibition in anti-estrogen-sensitive and resistant breast cancer cells. Br. J. Cancer *102*, 342–350.

Jorda, R., Buckova, Z., Reznickova, E., Bouchal, J., and Krystof, V. (2018). Selective inhibition reveals cyclin-dependent kinase 2 as another kinase that phosphorylates the androgen receptor at serine 81. Biochimica et biophysica acta. Molecular cell research *1865*, 354–363.

Kawakami, M., Mustachio, L.M., Liu, X., and Dmitrovsky, E. (2018). Engaging anaphase catastrophe mechanisms to eradicate aneuploid cancers. Mol. Cancer Ther. *17*, 724–731.

Kirchmair, J., Distinto, S., Liedl, K.R., Markt, P., Rollinger, J.M., Schuster, D., Spitzer, G.M., and Wolber, G. (2011). Development of anti-viral agents using molecular modeling and virtual screening techniques. Infect. Disord.: Drug Targets *11*, 64–93.

Kozyrska, K., Pilia, G., Vishwakarma, M., Wagstaff, L., Goschorska, M., Cirillo, S., Mohamad, S., Gallacher, K., Carazo Salas, R.E., and Piddini, E. (2022). p53 directs leader cell behavior, migration, and clearance during epithelial repair. Science *375*, eabl8876.

Kumarasamy, V., Vail, P., Nambiar, R., Witkiewicz, A.K., and Knudsen, E.S. (2021). Functional

determinants of cell cycle plasticity and sensitivity to CDK4/6 inhibition. Cancer Res. *81*, 1347–1360.

Leal-Esteban, L.C., and Fajas, L. (2020). Cell cycle regulators in cancer cell metabolism. Biochim. Biophys. Acta, Mol. Basis Dis. *1866*, 165715.

Li, J., Jiang, K., and Zhao, F. (2015). Icariin regulates the proliferation and apoptosis of human ovarian cancer cells through microRNA-21 by targeting PTEN, RECK and Bcl-2. Oncol. Rep. *33*, 2829–2836.

Li, S., Priceman, S.J., Xin, H., Zhang, W., Deng, J., Liu, Y., Huang, J., Zhu, W., Chen, M., Hu, W., et al. (2013). Icaritin inhibits JAK/STAT3 signaling and growth of renal cell carcinoma. PLoS One *8*, e81657.

Liang, J., Zubovitz, J., Petrocelli, T., Kotchetkov, R., Connor, M.K., Han, K., Lee, J.H., Ciarallo, S., Catzavelos, C., Beniston, R., et al. (2002). PKB/Akt phosphorylates p27, impairs nuclear import of p27 and opposes p27-mediated G1 arrest. Nat. Med. *8*, 1153–1160.

Mo, D., Zhu, H., Wang, J., Hao, H., Guo, Y., Wang, J., Han, X., Zou, L., Li, Z., Yao, H., et al. (2021). Icaritin inhibits PD-L1 expression by targeting protein IkappaB kinase alpha. Eur. J. Immunol. *51*, 978–988.

Otto, T., and Sicinski, P. (2017). Cell cycle proteins as promising targets in cancer therapy. Nat. Rev. Cancer *17*, 93–115.

Pierson-Mullany, L.K., and Lange, C.A. (2004). Phosphorylation of progesterone receptor serine 400 mediates ligand-independent transcriptional activity in response to activation of cyclin-dependent protein kinase 2. Mol. Cell Biol. *24*, 10542–10557.

Razavipour, S.F., Harikumar, K.B., and Slingerland, J.M. (2020). p27 as a transcriptional regulator: new roles in development and cancer. Cancer Res. *80*, 3451–3458.

Roskoski, R., Jr. (2019). Cyclin-dependent protein serine/threonine kinase inhibitors as anticancer drugs. Pharmacol. Res. *139*, 471–488.

Saeidnia, S., Gohari, A.R., and Manayi, A. (2016). Reverse pharmacognosy and reverse pharmacology; two closely related approaches for drug discovery development. Curr. Pharm. Biotechnol. *17*, 1016–1022.

Sánchez-Martínez, C., Lallena, M.J., Sanfeliciano, S.G., and de Dios, A. (2019). Cyclin dependent kinase (CDK) inhibitors as anticancer drugs: recent advances (2015-2019). Bioorg. Med. Chem. Lett. *29*, 126637.

Shin, I., Yakes, F.M., Rojo, F., Shin, N.Y., Bakin, A.V., Baselga, J., and Arteaga, C.L. (2002). PKB/Akt mediates cell-cycle progression by phosphorylation of p27(Kip1) at threonine 157 and modulation of its cellular localization. Nat. Med. *8*, 1145–1152.

Siegel, R.L., Miller, K.D., Fedewa, S.A., Ahnen, D.J., Meester, R.G.S., Barzi, A., and Jemal, A. (2017). Cancer statistics, 2017. CA. Cancer J. Clin. *67*, 177–193.

Siegel, R.L., Miller, K.D., and Jemal, A. (2019). Cancer statistics, 2019. CA. Cancer J. Clin. *69*, 7–34.

Spencer, S.L., Cappell, S.D., Tsai, F.C., Overton, K.W., Wang, C.L., and Meyer, T. (2013). The proliferation-quiescence decision is controlled by a bifurcation in CDK2 activity at mitotic exit. Cell *155*, 369–383.

Spring, L.M., Wander, S.A., Andre, F., Moy, B., Turner, N.C., and Bardia, A. (2020). Cyclin-dependent kinase 4 and 6 inhibitors for hormone receptor-positive breast cancer: past, present, and future. Lancet *395*, 817–827.

Starostina, N.G., and Kipreos, E.T. (2012). Multiple degradation pathways regulate versatile CIP/KIP CDK inhibitors. Trends Cell Biol. *22*, 33–41.

Sun, L., Peng, Q., Qu, L., Gong, L., and Si, J. (2015). Anticancer agent icaritin induces apoptosis through caspase-dependent pathways in human hepatocellular carcinoma cells. Mol. Med. Rep. *11*, 3094–3100.

Sung, H., Ferlay, J., Siegel, R.L., Laversanne, M., Soerjomataram, I., Jemal, A., and Bray, F. (2021). Global cancer statistics 2020: GLOBOCAN estimates of incidence and mortality worldwide for 36 cancers in 185 countries. CA. Cancer J. Clin. *71*, 209–249.

Tadesse, S., Anshabo, A.T., Portman, N., Lim, E., Tilley, W., Caldon, C.E., and Wang, S. (2020). Targeting CDK2 in cancer: challenges and opportunities for therapy. Drug Discov. Today *25*, 406–413.

Tadesse, S., Caldon, E.C., Tilley, W., and Wang, S. (2019b). Cyclin-dependent kinase 2 inhibitors in cancer therapy: an update. J. Med. Chem. *62*, 4233–4251.

Wang, L., Shao, X., Zhong, T., Wu, Y., Xu, A., Sun, X., Gao, H., Liu, Y., Lan, T., Tong, Y., et al. (2021). Discovery of a first-in-class CDK2 selective degrader for AML differentiation therapy. Nat. Chem. Biol. *17*, 567–575.

Wang, X.F., and Wang, J. (2014). Icaritin suppresses the proliferation of human osteosarcoma cells in vitro by increasing apoptosis and decreasing MMP expression. Acta Pharmacol. Sin. *35*, 531–539.

Yang, X.J., Xi, Y.M., and Li, Z.J. (2019). Icaritin: a novel natural candidate for hematological malignancies therapy. BioMed Res. Int. *2019*, 4860268.

Yin, X., Yu, J., Zhou, Y., Wang, C., Jiao, Z., Qian, Z., Sun, H., and Chen, B. (2018). Identification of CDK2 as a novel target in treatment of prostate cancer. Future Oncol. *14*, 709–718.

Yu, D.J., Li, Y.H., and Zhong, M. (2020). MicroRNA-597 inhibits NSCLC progression through negatively regulating CDK2 expression. Eur. Rev. Med. Pharmacol. Sci. *24*, 4288–4297.

Zhang, C., Chen, X., Liu, H., Li, H., Jiang, W., Hou, W., McNutt, M.A., Lu, F., and Li, G. (2015). Alpha fetoprotein mediates HBx induced carcinogenesis in the hepatocyte cytoplasm. Int. J. Cancer *137*, 1818–1829.

Zhang, C., Huang, J., and An, W. (2017). Hepatic stimulator substance resists hepatic ischemia/reperfusion injury by regulating Drp1 translocation and activation. Hepatology *66*, 1989–2001.

Zheng, Q., Liu, W.W., Li, B., Chen, H.J., Zhu, W.S., Yang, G.X., Chen, M.J., and He, G.Y. (2014). Anticancer effect of icaritin on human lung cancer cells through inducing S phase cell cycle arrest and apoptosis. J Huazhong Univ Sci Technolog Med Sci *34*, 497–503.

Zheng, X., Gou, Y., Jiang, Z., Yang, A., Yang, Z., and Qin, S. (2021). Icaritin-induced FAM99A affects GLUT1-mediated glycolysis via regulating the JAK2/STAT3 pathway in hepatocellular carcinoma. Front. Oncol. *11*, 740557.

STAR★METHODS

KEY RESOURCES TABLE

REAGENT or RESOURCE	SOURCE	IDENTIFIER
Antibodies		
Anti-GAPDH Rabbit pAb	Wanleibio	WL03301
Phospho-p27 Kip1 (Thr187) Polyclonal Antibody	invitrogen	PA5-104911; RRID: AB_2816384
Phospho-foxo1 (Ser249) Polyclonal Antibody	invitrogen	PA5-105996; RRID: AB_2817395
Rabbit polyclonal anti-p27 Rabbit polyclonal anti-CDK2 Mouse monoclonal anti-E2F Rabbit polyclonal anti-FOXO1 Rabbit polyclonal anti-Rb	proteintech	25614-1-AP; RRID: AB_2880161 10122-1-AP: RRID: AB_2078556 66515-1-Ig; RRID: AB_2881878 18592-1-AP; RRID: AB_10860103 10048-2-Ig; RRID: AB_2177320
Mouse monoclonal anti-CyclinE	Santa cruz	sc-377100; RRID: AB_2923122
Biological samples		
Heat-inactivated fetal bovine serum	Gibco	10100147C
Chemicals, peptides, and recombinant proteins		
DMEM medium	Gibco	11995–065
CDK2 inhibitor K03861	Selleck	S8100
BamH I EcoR I	NEB	#R3136V #R3101V
Mega Tran 2.0	Origene	TT210002
Annexin V, FITC Apoptosis Detection Kit	DOJINDO	AD10-DOJINDO
Experimental models: Cell lines		
PLC/PRF/5	National Institutes for Food and Drug Control	N/A
HT-29	Peking Union Medical College	N/A
Experimental models: Organisms/strains		
Mouse: athymic BALB/c CAnN.Cg-*Foxn1*^{nu}/Crl	Charles River Japan	401
Recombinant DNA		
PcDNA3.1-CDK2	This paper	N/A

RESOURCE AVAILABILITY

Lead contact

Further information and requests for resources and reagents should be directed to and will be fulfilled by the lead contact, Chao Zhang (zc_mdy@163.com).

Materials availability

This study did not generate new unique reagents.

Data and code availability

Data reported in this paper will be shared by the lead contact upon request. This paper does not report original code. Any additional information required to reanalyze the data reported in this paper is available from the lead contact upon request

EXPERIMENTAL MODEL AND SUBJECT DETAILS

Cell lines

PLC/PRF/5 and HT-29 cells were purchased from National Institutes for Food and Drug Control and Peking Union Medical College, respectively. All cells were maintained in a DMEM medium supplemented with 10% fetal calf serum (FCS) at 37°C in a humidified atmosphere with 5% CO2.

Animals

4-week-old athymic BALB/c male mice were maintained under specific pathogen-free conditions with a 12 h light-dark cycle. This study was performed under protocols approved by the Beijing Hospital Animal Care and Use Committee (Beijing, China).

METHOD DETAILS

Reverse virtual screening

The CDK2 protein structure was downloaded from the PDB database (PDB ID: 5JVP, 4ACM). The CDK2 protein binding pocket was generated using PyMOL software. Docking platform, powered with auto dock-vina at Beijing Beike Deyuan Bio-Pharm Technology Co. Ltd.

Cell-Derived Xenograft (CDX) model

An aliquot of 1×10^6 PLC/PRF/5 (5×10^5 HT-29) cells was suspended in 200 μL PBS and injected subcutaneously into the armpits of mice. 35 mg/kg body weight of icaritin was gavage administered after the inoculation of tumor cells. The length and width of tumors were measured once they could be palpated, and tumor volume was calculated using the formula, $V = 0.52 \times L \times W^2$ (n = 10 for each group).

Surface plasmon resonance (SPR)

Equilibrium dissociation constant (K_D) values were measured by SPR method using Biacore 8K, according to USP (United States Pharmacopeia) General Information/(1105) Immunological Test Methods-Surface Plasmon Resonance (2016). CDK2 was diluted to 60 μg/mL, and approximately 10,000 RU of the coupled protein was obtained. Icaritin with a maximum of 25μM was used. The final reaction buffer containing 4.5% DMSO was gradiently diluted to obtain ligand compounds with different concentration gradients. A simple one-to-one Langmuir combination model was used to calculate the association rate (k_{on}) and dissociation rate (k_{off}) by simultaneously fitting the association and dissociation sensorgrams. K_D was calculated as the ratio of k_{off}/k_{on}.

Histology staining

Tumor tissues (5-μm) were stained with hematoxylin and eosin (H&E) and photographed by light microscopy (DM5000 B; Leica Microsystems, Wetzlar, Germany). Immunohistochemical staining was carried out following a standard protocol. Quantitative results were calculated by Image-Pro Plus software to average the positive area density of P27 and CDK2 for 5 fields in each section.

Plasmid transfection

PcDNA3.1-CDK2 was constructed with BamH I/EcoR I. All the plasmids used in these transfection experiments were prepared using a Large-scale Purification Kit (Tiangen Biotech, Beijing, China), following the manufacturer's recommended protocol. Cells were transfected with plasmid using Mega Tran 2.0 (Origene, Wuxi, Jiangsu, China), following the application guide of the product.

Reverse transcription and quantitative real-time PCR (RT-qPCR)

Expression of FOXO1, CyclinE, CDK2, P27, FasL, Bim and TRAIL mRNA were evaluated by the RT-qPCR assay as previously described (Zhang et al., 2017). Relative concentrations of mRNAs are presented as mean fold-change of samples compared to the control. Reverse transcription of miRNAs was carried out with commercial primers (TransGene Biotech, Beijing, China). For analysis of miR-597 expression, qPCR analyses were conducted using TransStart Green qPCR SuperMix (TransGene Biotech, Beijing, China) and data were normalized to the expression of U6. Primers used for qRT-PCR are listed in Table S3.

Western blotting

Western blotting was performed for analyses of the expression of FOXO1, CyclinE, CDK2 and P27 in tumor tissues and cell lines as previously described (Zhang et al., 2015). Primary antibodies against Pan Phospho-Serine/Threonine (Abmart, China), $FOXO1^{ser249}$, $P27^{Thr187}$ (Invitrogen, USA), FasL, Bim, TRAIL, GAPDH (Wanleibio, China), FOXO1, CyclinE, CDK2, P27, E2F, Rb (proteintech, USA) were used.

Coimmunoprecipitation (CoIP)

The interaction of CyclinE/CDK2 and E2F1/Rb in cell lines and tumor tissues was evaluated by CoIP assay. Lysates were clarified by centrifugation and then incubated overnight at 4°C with an antibody against CyclinE (or CDK2, proteintech, USA) bound to protein A-Sepharose. Non-immune rabbit IgG was used as a control. Immune complexes were eluted for SDS–PAGE electrophoresis and Western blot analysis.

Cell nuclei staining for apoptosis

Laser confocal microscopy was performed to evaluate the apoptosis induced by icaritin. Cell nuclei were labeled with DAPI (Life, Oregon, USA). Cells were viewed and captured with a Laser Confocal Microscope (Leica TCS-NT SP8, Germany).

Determination of cell viability

The effect of icaritin on cell viability was assessed using a Cell Counting Kit (CCK)-8 (Dojindo Laboratories, Kumamoto, Japan). The viability of cells was detected on a Universal Microplate Reader (EL X 800) at 450 nm. The cell viability with each treatment was calculated as % cell inhibition = $[(A_{450}$ sample - A_{450} background)/(A_{450} control - A_{450} background)] × 100%.

Flow cytometric analysis for apoptosis

Apoptosis induced by icaritin, icaritin + vector, and icaritin + CDK2 was analyzed by flow cytometry. Relative fluorescence intensities were measured by using a FACScan-420 flow cytometry instrument (Becton-Dickinson) with excitation at 488 nm and emission at 598 nm. The extent of apoptosis of cells was determined according to DNA analysis. The fluorescence signals of apoptotic cells were represented by Annexin V+/PI− (early apoptosis) and Annexin V+/PI+ (late apoptosis/necrosis).

Flow cytometric analysis for cell cycle

Changes in cell cycle distribution were analyzed by flow cytometry. After linear amplification, PI fluorescence was collected with a 575/25 nm bandpass filter (FL2). Data from 10,000 to 20,000 single cell events were collected for each measurement, while cell doublets and aggregates were gated out using a two-parameter histogram of FL2-Area versus FL2-Width. Cell cycle histograms were analyzed using ModFit LT™ 3.0 software packages.

EdU incorporation assay

The proliferation of cancer cells (Huh7, MCF-7, Hela et al.) was determined using the Cell-Light™ EdU Apollo®488 *In Vitro* Imaging Kit (RiboBio Co., Ltd. Guangzhou, China), according to the manufacturer's protocol. Cells were incubated with 50 μM 5-ethynyl-2′-deoxyuridine (EdU) and cell nuclei were stained with Hoechst 33342. The fluorescent images were observed on Operetta™ (a high throughput imaging system) at 340 and 488 nm.

TUNEL staining for apoptosis

The terminal deoxynucleotidyl transferase (dUTP)-mediated nick end-labeling (TUNEL) assay was carried out according to the manufacturer's protocol with an *in situ* cell death/apoptosis detection kit (Roche Diagnostics, Mannheim, Germany). The results were scored semiquantitatively by averaging the numbers of TUNEL-positive cells per low-power field (LPF) for 5 fields in each experiment.

QUANTIFICATION AND STATISTICAL ANALYSIS

The results of multiple observations are presented as the mean ± s.d. of at least three separate experiments. Statistical significance was determined using the Student's *t* test (SPSS 19.0 software). p values less than 0.05 were considered statistically significant.